


RESEARCH

Open Access



# In vitro anticancer activity of folate-modified docetaxel-loaded PLGA nanoparticles against drug-sensitive and multidrug-resistant cancer cells

Yuri I. Poltavets<sup>1</sup>, Alexander S. Zhirnik<sup>1</sup>, Vasilisa V. Zavarzina<sup>1</sup>, Yuliya P. Semochkina<sup>1</sup>, Valentina G. Shuvatova<sup>1</sup>, Anna A. Krashenninnikova<sup>1</sup>, Sergey V. Aleshin<sup>1</sup>, Danil O. Dronov<sup>1</sup>, Eugeny A. Vorontsov<sup>1</sup>, Vadim Yu. Balabanyan<sup>2</sup> and Galina A. Posypanova<sup>1\*</sup> 

\*Correspondence:  
galinapo@gmail.com  
<sup>1</sup> National Research Centre  
"Kurchatov Institute",  
Moscow 123182, Russia  
Full list of author information  
is available at the end of the  
article

## Abstract

**Background:** Poly(lactic-co-glycolic acid) (PLGA) is a biodegradable and biocompatible polymer which is widely used as a matrix to incorporate therapeutic agents. The anticancer activity of targeted folate-modified docetaxel-loaded PLGA nanoparticles (F-NP-Doc) was studied in vitro.

**Methods:** Nanoparticles were prepared by a single-emulsion solvent-evaporation technique and characterized by physico-chemical methods. Cell survival was measured by the MTT assay and the sulforhodamine B assay. Folate receptor  $\alpha$  expression, particle uptake and apoptosis were assessed by flow cytometry.

**Results:** Folate-modified docetaxel-loaded PLGA nanoparticles showed high anticancer activity in vitro against HeLa cervical carcinoma cells and MCF7 breast adenocarcinoma cells overexpressing folate receptors. Targeted F-NP-Doc nanoparticles were more active compared to free docetaxel and non-targeted NP-Doc nanoparticles; in contrast, the activity of targeted nanoparticles against human fibroblasts (negative control) was significantly lower. F-NP-Doc particles, like free docetaxel, induced apoptosis in cancer cells. F-NP-Doc, but not unmodified docetaxel-loaded PLGA nanoparticles, reversed multidrug resistance of MCF7<sup>R</sup> breast adenocarcinoma cells. High antitumor activity of F-NP-Doc has also been proven in in vivo experiments.

**Conclusions:** The summarized experimental data brought us to the conclusion that the incorporation of docetaxel into the targeted PLGA nanoparticles dramatically improves its selectivity against cancer cells.

**Keywords:** PLGA nanoparticles, Docetaxel, Folic acid, Targeted delivery



## Background

Low selectivity of anticancer drugs results in a high incidence of side effects and remains one of the major problems in cancer chemotherapy. The high toxicity of anticancer drugs against proliferating cells is responsible for developing of numerous serious complications of hematopoietic system, gastrointestinal tract, immune and nervous systems. Over the past 3 decades, the targeted anticancer drugs have been actively developed to eliminate cancer cells. Targeted delivery of anticancer therapeutics is achieved by adding vector molecules to their composition. Such vector molecules include natural or synthetic ligands of receptors preferentially expressed in cancer cells, antibodies to these receptors, and aptamers. The interaction between vector and specific receptor triggers receptor-mediated endocytosis of targeted anticancer drug, thus increasing its selectivity.

Receptor-mediated endocytosis is an extremely effective cellular mechanism for rapid and controlled uptake of specific extracellular macromolecules such as low-density lipoproteins, growth factors, transport proteins as well as some low-molecular weight compounds, for example, folic acid (FA) (Bareford and Swaan 2007). FA is a low-molecular weight physiological ligand, which is non-immunogenic, inexpensive, stable, and readily available, and can be easily conjugated to other molecules through its carboxyl group. These properties have made FA one of the most popular ligands for targeted drug delivery. Actually, the unique properties of FA enable it to be near ideal vector for targeted liposomes, nanoparticles, quantum dots (Syu et al. 2012; Ye et al. 2014; Parveen and Sahoo 2010; Suriamoorthy et al. 2010; Chattopadhyay et al. 2013). This approach offers an opportunity to significantly enhance the efficacy of anticancer drugs. For example, the use of FA for targeted delivery of paclitaxel-loaded nanoparticles (Wang et al. 2012; Wu et al. 2012) resulted in a decrease in systemic toxicity and an increase in antitumor activity of the drug compared with free paclitaxel.

Poly(lactic-co-glycolic acid) (PLGA) is a biodegradable and biocompatible polymer which is widely used as a matrix to incorporate a wide range of therapeutic agents, including hydrophilic and hydrophobic small molecules, nucleic acids, proteins, etc. (Kapoor et al. 2015). PLGA is approved by the Food and Drug Administration (FDA) and European Medicines Agency (EMA) for use in pharmaceutical products. Incorporation of poorly soluble cytostatic agents such as taxanes into polymeric nanoparticles is probably the most effective and simplest way to increase their therapeutic efficacy. At present, paclitaxel and docetaxel are widely used in the clinic to treat a variety of malignancies (Eisenhauer and Vermorken 1998; Montero et al. 2005). Both drugs exert cytostatic activity against cancer cells by binding to beta-tubulin and stabilizing cytoskeleton microtubules, resulting in cell cycle arrest at the G2/M phase, inhibition of mitosis and subsequent cell death (Hernandez-Vargas et al. 2007; Kraus et al. 2003). A serious disadvantage of taxanes is their extremely low solubility in aqueous solutions. When used in the clinic, solubilizers, such as Cremophor<sup>®</sup> EL for paclitaxel or polysorbate-80 for docetaxel, have to be added. These solubilizers often cause serious allergic and toxic reactions that limit the use of the drugs.

The aim of this study was to prepare targeted folate-modified docetaxel-loaded PLGA nanoparticles, to evaluate their cytostatic activity against human cancer cell

lines in comparison with that of docetaxel, and to study the activity of targeted nanoparticles against cancer cells with multidrug resistance phenotype.

## Methods

### Materials

50/50 poly(D,L-lactic-co-glycolic acid), ester terminated (PLGA 50:50), PURAC PDLG 5004 (inherent viscosity 0.41 dl/g) was purchased from Purac Biomaterials (Netherlands); docetaxel trihydrate, pharm. EP 7.5 (Doc) was purchased from QUILU Pharmaceutical Co. Ltd. (China); polyvinyl alcohol (PVA), 87–90% hydrolyzed, average mol wt 30,000–70,000, was purchased from Sigma-Aldrich (USA); dimethyl sulfoxide (DMSO), methylene chloride, and puriss. (MeCl<sub>2</sub>) were purchased from Chimmed (Russia); folic acid–dodecylamine (FoAD) was kindly provided by IREA Institute (Moscow, Russia, <http://www.irea.org.ru>). Acetonitrile used as the mobile phase in high-performance liquid chromatography (HPLC) was purchased from Macron (Poland). All other chemicals used were of reagent grade. DMEM culture medium, trypsin–EDTA, gentamicin, and rabbit polyclonal antibodies against the folate receptor  $\alpha$  were purchased from Thermo Fisher Scientific (USA). Fetal bovine serum (FBS) was obtained from HyClone (USA). Alexa Fluor<sup>®</sup> 488-conjugated goat anti-rabbit secondary antibodies were purchased from Abcam (USA). FITC Annexin V Apoptosis Detection Kit with PI was obtained from BioLegend (USA). Other reagents were purchased from Sigma-Aldrich (USA).

### Preparation of polymeric nanoparticles (NP–Doc, F–NP–Doc, F–NP–FDA)

PLGA nanoparticles were prepared using a single-emulsion solvent-evaporation method. All phases were filtered through 0.45- $\mu$ m nylon membrane filters before use. The polymeric nanoparticles (NPs) were formulated by mixing of Doc (NP–Doc), FoAD and Doc (F–NP–Doc), FoAD and fluorescein diacetate (F–NP–FDA) with PLGA 50:50 solution in MeCl<sub>2</sub>. This organic phase was mixed with aqueous PVA solution and sonicated on ice. We used the Sonics Vibra-Cell VCX 750 sonicator (Sonics & Materials Inc., USA) equipped with #630-0220 probe and #630-0420 microtip with 6 mm tip diameter. Sonication was performed in 100-mL glass beaker using the following settings: energy—45 J, probe amplitude—45% (108  $\mu$ m), pulsation (pulse/clear)—2 s/2 s, sonication time: 1-min sonication (2-min overall pulse/clear)—1-min rest—1-min sonication (2-min overall pulse/clear). MeCl<sub>2</sub> was evaporated from obtained emulsion at room temperature for 12–16 h with constant stirring. Suspension of polymeric particles was centrifuged (30,000g, 4 °C) and resuspended in water with addition of D-mannitol. Suspension with additive was freeze-dried and stored in refrigerator (4 °C) before use.

### Preparation of NP–Doc

5.0 mg of Doc and 100.0 mg of PLGA 50:50 were dissolved in 2.5 mL of MeCl<sub>2</sub> and mixed with 17.5 mL of 1.0% PVA solution, then processed as described above. 50.0 mg of D-mannitol was added to the suspension before lyophilization.

### Preparation of F–NP–Doc

0.2 mg of FoAD, 10.0 mg of Doc, and 200.0 mg of PLGA 50:50 were dissolved in 5.0 mL of MeCl<sub>2</sub> and mixed with 35.0 mL of 1.0% PVA solution, then processed

as described above. 70.0 mg of D-mannitol was added to the suspension before lyophilization.

#### ***Preparation of F-NP-FDA***

2.0 mg of FDA and 200.0 mg of PLGA 50:50 were dissolved in 5.0 mL of MeCl<sub>2</sub> and mixed with 20.0 µL of FoAD solution in MeCl<sub>2</sub> (5 mg/mL). This organic phase was added to 35.0 mL of 0.25% PVA solution and then processed as described above. D-Mannitol was added to the suspension before lyophilization. FDA content was determined by UV spectroscopy at 209 nm.

#### **Characterization of NPs**

##### ***Particle size analysis and zeta potential measurements***

The mean hydrodynamic diameter (Z-average), particle size distribution and polydispersity index (PDI) were measured by dynamic light scattering. Zeta potentials were determined by electrophoretic light scattering using Zetasizer Nano ZS ZEN 3600 (Malvern Instruments Ltd., UK) at 25 °C. The NP samples were prepared in deionized water at a concentration of about 0.2 mg NP/mL and measured in triplicates.

##### ***Determination of docetaxel loading***

Lyophilized NP-Doc and F-NP-Doc nanoparticles were dissolved in DMSO, and Doc content was measured using the Agilent 1200 HPLC system with a UV detector (Agilent Technologies, USA). Chromatographic separation was performed on a reverse-phase column Agilent ZORBAX Eclipse XDB-C18, 250 × 4.6 mm, 5 µm, thermostated at 30 °C. Flow rate: 1.2 mL/min. Chromatography was carried out in the gradient conditions: phase A—water, phase B—acetonitrile. Gradient was programmed as follows: isocratic 72% A, 28% B (0–9 min), then linear (9–30 min) from 72% A, 28% B to 28% A, 72% B, then linear back to 72% A, 28% B (30–50 min). The Doc peak was measured at a wavelength of 290 nm and quantitatively determined by comparing with a standard curve. Approximate retention time for Doc was about 27 min.

##### ***Particle morphology examination***

The morphological examination of NPs was performed by transmission electron cryomicroscopy (TEM). The samples were diluted in 1.0 mL of purified water, vortexed for 1 min and placed on previously hydrophilized supporting mesh. After vitrification in liquid ethane, the samples were transferred in liquid nitrogen to the pressing station and then placed in a cassette holder under cryogenic conditions. Imaging was performed using Titan Krios TEM FEI (Thermo Fisher Scientific, USA) at 5000×–18,000× magnification in a low-dose mode using a Falcon II electron detector.

##### ***In vitro docetaxel release studies***

In vitro drug release study was performed using dialysis method. 1.0 mL of NP suspension containing 77.85 mg of NPs was placed into the dialysis membrane tubings OrDial D14 (Orange Scientific, Belgium) with pore diameter of 12–14 kDa and dialyzed against 2000 mL of phosphate buffered saline (PBS), pH 7.4, containing 0.5%

Tween 80 at 37 °C on an orbital shaker stirring at a rate of 50 rpm. At the indicated times (the total incubation time was 48 h), the samples were quantitatively transferred from dialysis bags to glass vials, frozen, and lyophilized. Docetaxel loading in the lyophilized samples was determined by HPLC. Time-dependent curve of docetaxel release from polymeric nanoparticles was built according to the obtained results.

#### Cell lines

HeLa human cervical carcinoma cells, MDA-MB-231 human breast adenocarcinoma cells and LECH human embryonic lung fibroblasts were obtained from the Russian collection of cell cultures (St. Petersburg, Russia). MCF7<sup>R</sup> human breast adenocarcinoma cells and SKOV3 human ovarian carcinoma cells were kindly provided by Dr. V. Yu. Alakhov (Supratek Pharma Inc. Quebec, Canada). MCF7 human breast adenocarcinoma cells were purchased from the American Type Culture Collection (ATCC). Cells were maintained in plastic flasks (Corning, USA) in DMEM medium supplemented with 10% FBS and 50 µg/mL gentamicin in a CO<sub>2</sub> incubator at 37 °C in a humidified atmosphere containing 5% CO<sub>2</sub>. Cells were passaged twice a week using trypsin–EDTA solution.

#### Evaluation of folate receptor α expression

The folate receptor expression levels in cells were assessed by flow cytometry. Cells were harvested using trypsin–EDTA solution, washed once with PBS and fixed with 2% para-formaldehyde. Fixed cells were permeabilized with 0.3% Triton X-100, blocked with 2% fatty acid-free bovine serum albumin (BSA) in PBS and incubated with rabbit polyclonal antibodies against folate receptor α (1:200 dilution) in blocking buffer for 1 h. After washing, the cells were incubated in blocking buffer with Alexa Fluor 488-labeled secondary antibodies (1:200 dilution). Afterwards, cells were washed, resuspended in PBS and analyzed on a BD FACSCalibur flow cytometer (BD Biosciences, USA). 10<sup>4</sup> cells were analyzed in each sample. The staining index (SI) was calculated according to the formula:

$$SI = \frac{MF_{Ist} - MF_{Ia}}{2 \times SDa},$$

where MF<sub>Ist</sub> and MF<sub>Ia</sub> are medium fluorescence intensity of stained cells and an auto-fluorescence, respectively; SDa is standard deviation of the MF<sub>Ia</sub>.

#### In vitro cellular uptake study

HeLa cells were seeded onto coverslips in 24-well plates 1 day prior to the experiment for attachment and adaptation. Cells were incubated with F–NP–FDA (12 µM in fluorescein diacetate equivalent) for 1 h in folic acid-free DMEM supplemented with 0.1% BSA in a CO<sub>2</sub> incubator under standard conditions. At the end of incubation, cells were washed three times with PBS and analyzed on a BD FACSCalibur flow cytometer equipped with a 488-nm argon laser in the fluorescence channel FL1 or Axiovert 40 CFL fluorescence microscope (Carl Zeiss, Germany). To disclose the potential mechanisms of nanoparticle uptake, the endocytosis inhibitors including genistein (1 µg/mL, caveolae-mediated endocytosis inhibitor), monodansylcadaverine (300 µM, clathrin-mediated endocytosis

inhibitor) and amiloride (1.25 mM, macropinocytosis inhibitor) were added to HeLa cells 30 min prior to incubation with F-NP-FDA.

#### Evaluation of cytotoxic activity of NPs

Cells were seeded in folic acid-free DMEM supplemented with 10% FBS and 50 µg/mL gentamicin in 96-well plates 1 day prior to the experiment for attachment and adaptation. Docetaxel and nanoparticles were added in a wide range of concentrations in triplicates for each concentration and incubated under standard conditions for 24–72 h. Cell survival was measured by the MTT assay (Alley et al. 1988) and the sulforhodamine B (SRB) assay (Skehan et al. 1990). *MTT assay*. 2 h before the end of incubation, 50 µL of MTT at a concentration of 1 mg/mL in culture medium was added to each well. After color development, the medium was removed, the precipitated formazan crystals were dissolved in 150 µL of DMSO, and the color intensity was measured by absorbance at 570 nm using an iMark microplate absorbance reader (Bio-Rad, USA). *SRB assay*. After the end of incubation, the medium was removed, and the cells were fixed with 10% trichloroacetic acid (TCA) for 1 h. Then TCA was removed, and the samples were dried in air and stained for 30 min with SRB solution (0.4% SRB in 1% acetic acid). Next, the plates were washed five times with 1% acetic acid and dried in air, and protein-bound SRB was dissolved in unbuffered 10 mM Tris (pH 10.5). The color intensity was measured by absorbance at 570 nm on a microplate reader. Cell survival was assessed as a percentage of the untreated control.

#### Quantitation of apoptosis by flow cytometry

HeLa cells were seeded in six-well plates (Corning, USA) 1 day prior to the experiment and cultured in FA-free DMEM supplemented with 10% FBS and 50 µg/mL gentamicin. On the day of the experiment, the culture medium was replaced with fresh medium containing docetaxel and polymeric nanoparticles in concentration of 2.5 and 10 nM in docetaxel equivalent. After the incubation was completed, cells were harvested using trypsin–EDTA, washed twice in PBS and stained with FITC Annexin V Apoptosis Detection Kit with PI according to the manufacturer's instructions. Cells were incubated for 15 min in a staining buffer containing Annexin V-FITC and propidium iodide. Samples were analyzed without washing on a BD FACSCalibur flow cytometer in the fluorescence channels FL1 (for FITC) and FL2 (for PI).

#### In vivo anticancer activity of F-NP-Doc

All animal studies were conducted according to the European Convention for the Protection of Vertebrate Animals (Strasbourg 1986). The protocols of this study and experimental procedures were approved by the Ethical Committee of the National Research Center “Kurchatov Institute”. Specific pathogen-free (SPF) female C57BL/6 mice were obtained from Pushchino Nursery of Laboratory Animals (Pushchino, Russia). Ca755 mammary adenocarcinoma cells ( $1 \times 10^6$ ) were injected subcutaneously into the right flank of each animal (the day of tumor implantation was designated as day 0). The mice were randomized into vehicle control (saline) and treatment groups ( $n=9$  per group), and the treatments were started 48 h after tumor implantation. Docetaxel was dissolved in Tween 80/ethanol/saline (PRODUCT MONOGRAPH, Taxotere®), and F-NP-Doc

was dissolved in saline. Drugs at a dosage of 15 mg/kg/dose in 0.4 mL of corresponding solvent were intravenously administered via the lateral tail vein on 3, 6 and 9 days after tumor inoculation. Tumor sizes were measured every 2–3 days, and tumor volume ( $V$ ,  $\text{mm}^3$ ) was calculated using the formula:

$$V = a^2 \times b/2,$$

where  $a$  and  $b$  refer to the short and long diameters of tumor, respectively.

The tumor growth inhibition (TGI) was calculated using the formula:

$$\text{TGI}(\%) = (V_C - V_T)/V_C \times 100,$$

where  $V_c$  and  $V_t$  refer to the mean tumor volume in control and experimental groups, respectively.

### Statistical analysis

Plotting and statistical data processing were performed using OriginPro 8.5 (OriginLab Corporation) and Microsoft Excel (Microsoft Corporation). The accuracy of the results was evaluated using the Student's  $t$ -test. The data in the tables and graphs are presented as an average of at least three experiments  $\pm$  SE.

## Results and discussion

### Characterization of nanoparticles

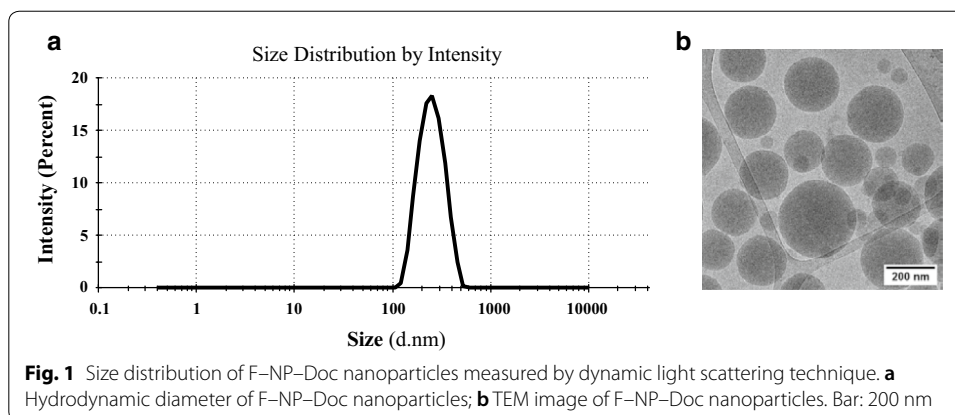
Folate-modified docetaxel-loaded polymeric nanoparticles (F-NP-Doc), docetaxel-loaded nanoparticles without FA (NP-Doc), and functionalized fluorescein diacetate-loaded particles (F-NP-FDA) were formulated by a single-emulsion solvent-evaporation method using an ultrasonic homogenizer. A folate-dodecylamine conjugate (FoAD) was used to prepare F-NP-Doc particles. FoAD contains both hydrophilic and hydrophobic groups, has amphiphilic properties and can act as a surfactant. The use of FoAD contributes to the localization of the vector FA moiety on the surface of F-NP-Doc and F-NP-FDA. The particles were lyophilized and stored at 4 °C.

The properties of the nanoparticles (for resuspended lyophilizates) are presented in Table 1. The results of the quantitative analysis of docetaxel and FDA are given for a dry matter.

TEM micrograph (Fig. 1b) clearly shows that the prepared nanoparticles have a regular spherical shape. The average diameter of docetaxel-loaded PLGA particles measured by dynamic light scattering was about 230 nm (Table 1, Fig. 1a); fluorescein diacetate-loaded PLGA particles had a slightly greater diameter—263 nm.

**Table 1 Physicochemical parameters of the docetaxel-loaded and fluorescein diacetate-loaded PLGA nanoparticles**

Sample	Z-average size, nm	Zeta potential, mV	Polydispersity index (Pdl)	The content of docetaxel (1) or fluorescein diacetate (2) in the sample, %
NP-Doc	231.2 $\pm$ 4.6	−4.88 $\pm$ 0.41	0.091 $\pm$ 0.09	2.32 $\pm$ 0.07 (1)
F-NP-Doc	227.6 $\pm$ 5.9	−3.75 $\pm$ 0.29	0.068 $\pm$ 0.015	3.13 $\pm$ 0.10 (1)
F-NP-FDA	263.1 $\pm$ 6.2	−6.85 $\pm$ 0.24	0.075 $\pm$ 0.020	0.141 $\pm$ 0.009 (2)



The dimensions of prepared nanoparticles ranged from 100 to 400 nm (Fig. 1a). Using Zetasizer Software 7.11 (Malvern Instruments, UK), we calculated that 25% of particles were less than 200 nm, 27% of particles had a size in the range of 300–400 nm, and 48% of particles had a size in the range of 200–300 nm. A number of studies have shown that 50–100 nm is the optimal size of particles for effective cellular endocytosis (in vitro) (Liu et al. 2013; Huang et al. 2010; Lu et al. 2009; Hoshyar et al. 2016). However, the results obtained by many researchers suggest that, unlike unmodified particles, targeted particles with a diameter of 200–300 nm are also effectively internalized into cancer cells (Yu et al. 2011). Clear evidence on the cellular uptake of relatively large (216 nm and 500 nm) transferrin-conjugated targeted particles through clathrin-dependent receptor-mediated endocytosis was provided by Tsuji et al. (2013). Using confocal laser scanning microscopy and transmission electron microscopy, the authors have shown that the internalization of such particles was accompanied by the formation of large clathrin-coated vesicles even though their diameter was more than 500 nm and despite the fact that clathrin-coated vesicles have a diameter of 100 nm. These findings suggest that signals for internalization generated by stimulated receptors activate clathrin-mediated endocytosis preferentially. Additionally, larger transferrin-conjugated particles delivered drugs to cancer cells more selectively than their smaller counterparts. Based on the attained results, the authors concluded that large nanoparticles could be very good drug carriers in terms of their capacity and selective internalization into cancer cells even though particles are larger than normal clathrin-coated vesicles.

#### In vitro drug release study

The study of docetaxel release from polymeric nanoparticles in vitro was carried out under conditions of equilibrium dialysis at 37 °C in buffer (PBS) with pH 7.4. The ratio of nanoparticle mass to buffer volume was calculated without exceeding the solubility limit of docetaxel (8.7 μM) (Gurski et al. 2009). The quantitative HPLC analysis of Doc content in F-NP-Doc nanoparticles showed that 11.3% of initial amount of docetaxel in the sample (taken as 100%) was released within the first hour, which may be due to partial localization of the drug on the nanoparticles' surface.

Afterwards, the docetaxel release proceeded rather slowly (Fig. 2), that is only  $19.53 \pm 1.91\%$  and  $28.61 \pm 2.74\%$  of the drug was released within 24 and 48 h of incubation, respectively. Since the degradation rate of PLGA in PBS is very slow, as repeatedly



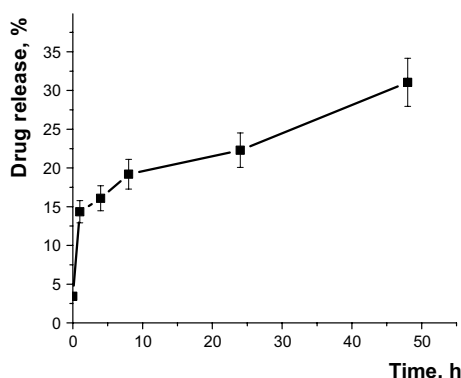


**Fig. 2** The release profile of docetaxel from F-NP-Doc nanoparticles at 37 °C (the initial amount of docetaxel in the sample was taken as 100%)

reported (Kamaly et al. 2016), docetaxel release is most likely to be due to the diffusion of the drug through a carrier matrix.

Diffusion of drug, erosion and swelling of polymer matrix and degradation of polymer are the main mechanisms for drug release. Since the degradation of PLGA is slow, the release of docetaxel from the nanoparticles would mainly depend on the drug diffusion and the matrix erosion.

In this study, slightly less than 30% of docetaxel was released from NPs to PBS for period studied (48 h). The faster release of docetaxel from particles takes place in living organism, as was shown by Mohammad and Reineke (2013). In general, biodegradation of PLGA occurs due to autocatalyzing hydrolysis of ester bonds to form oligomers and monomers of D,L-lactic and glycolic acids (Li 1999). Relatively small long-chain motifs generated at the initial stage undergo further hydrolytic cleavage to form shorter fragments and eventually lactic and glycolic acids which enter the Krebs's cycle, and are metabolized into carbon dioxide and water. Biodegradation of PLGA may also occur via enzymatic cleavage. Mammalian serine proteases,  $\alpha$ -chymotrypsin in particular, are able to hydrolyze ester bonds of PLGA (Lim et al. 2005). Other enzymes, including esterase, carboxypeptidase A and proteinase K, may participate in the biodegradation.

#### Immunocytochemical analysis of folate receptor $\alpha$ expression

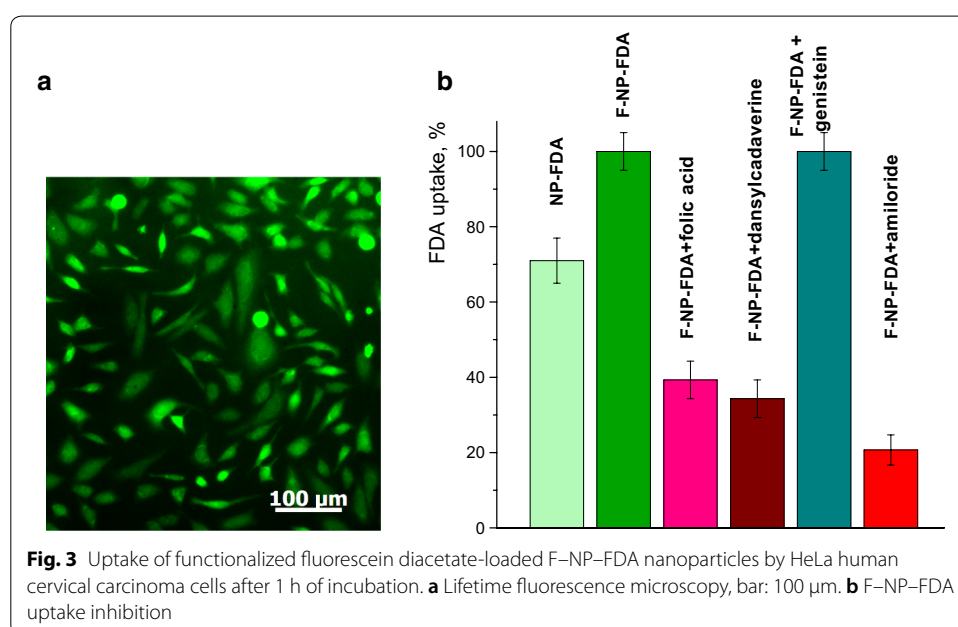
Before studying the in vitro anticancer activity of the prepared nanoparticles, we analyzed the folate receptor  $\alpha$  (FR) expression in cancer and control cells. The study of the FR content was performed by indirect immunochemical staining with subsequent detection of fluorescence using a BD FACSCalibur flow cytometer. The highest expression level of FR was found in HeLa cells (Table 2). In MCF7, MCF7<sup>R</sup> and SKOV3 cells, the content of the FR was slightly lower, but, nevertheless, significantly exceeded that in the control LECH cell line (human embryonic lung fibroblasts) and MDA-MB-231 cancer cell line (mammary adenocarcinoma).

#### Internalization of functionalized F-NP-FDA nanoparticles

Fluorescein diacetate (FDA) is nonfluorescent derivative of fluorescein penetrating the cell membrane due to its lipophilic nature. Being inside the cell, FDA is hydrolysed by

**Table 2** Expression of folate receptors in human cancer cells (HeLa, MCF7, MCF7<sup>R</sup>, MDA-MB-231, SKOV3, Ca755) and normal cells (LECH)

Cell line	Staining index (SI)
HeLa	31.7
MCF7	27.9
MCF7 <sup>R</sup>	20.4
MDA-MB-231	7.5
SKOV3	21.9
LECH	5.3
Ca755	21.9



intracellular esterases to form fluorescein. Thus, by measuring the intracellular fluorescence after incubation of cells with FDA-loaded nanoparticles, it is possible to determine the efficiency of their uptake. We compared the fluorescence intensity of cells incubated with targeted F-NP-FDA and non-targeted NP-FDA for 1 h at 37 °C (Fig. 3). The use of FDA allowed us to accurately measure the actual endocytosis rate of F-NP-FDA, since the interaction between polymer particles and cell membrane proceeds much more rapidly at 37 °C compared to 4 °C (data not shown; PLGA particles covalently linked to fluorescein were used in this set of experiments).

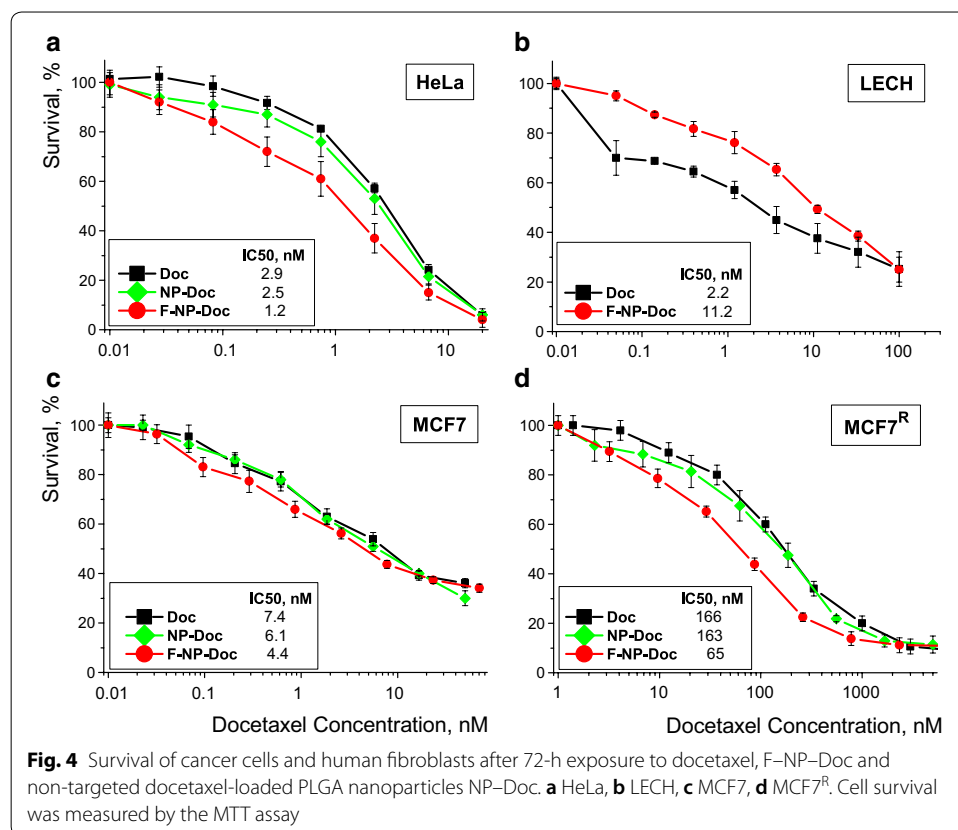
Fluorescence microscopy (Fig. 3a) and flow cytometry were used to investigate the internalization of fluorescein diacetate-loaded F-NP-FDA nanoparticles in HeLa cells. The obtained results indicate high accumulation of F-NP-FDA nanoparticles in cancer cells after 1 h of incubation at 37 °C.

But, it should be noted that internalization of nanoparticles may occur through various pathways (in turn, time needed for internalization may vary) depending on the size and shape of nanoparticles and the polymer properties. We found that the

use of F-NP-FDA functionalized particles significantly improved the efficiency of intracellular FDA accumulation: upon incubation of HeLa cells with FDA and F-NP-FDA at a concentration of  $12\ \mu\text{M}$  for 1 h at  $37\ ^\circ\text{C}$ , the MFI values were  $147 \pm 5$  and  $1249 \pm 27$  relative units, respectively. To elucidate the exact mechanisms of cellular uptake of F-NP-FDA, we performed the inhibition study using pathway-specific inhibitors. The use of endocytosis inhibitors is a common method to determine the nanoparticle entry route. Simultaneous exposure of cells to F-NP-FDA and monodansylcadaverine led to the inhibition of nanoparticle endocytosis by 66% (Fig. 5b). Genistein, an inhibitor of caveolae-mediated endocytosis, did not affect the cellular uptake of F-NP-FDA, while amiloride, an inhibitor of macropinocytosis, suppressed the endocytosis of F-NP-FDA by 80%. These results suggest that the main mechanisms by which F-NP-Doc internalize into cells are clathrin-dependent endocytosis and macropinocytosis.

#### Cytostatic activity of targeted docetaxel-loaded PLGA nanoparticles in vitro

Both targeted F-NP-Doc polymeric nanoparticles and free docetaxel dramatically inhibited cancer cell growth in vitro (Fig. 4) and induced apoptosis as early as 8 h after exposure (Fig. 5). The  $\text{IC}_{50}$  value of F-NP-Doc for HeLa cells highly expressed folate receptor was significantly lower than that of free docetaxel, indicating the higher cytostatic activity of the NPs prepared. Cell survival data obtained after 24 and 48 h



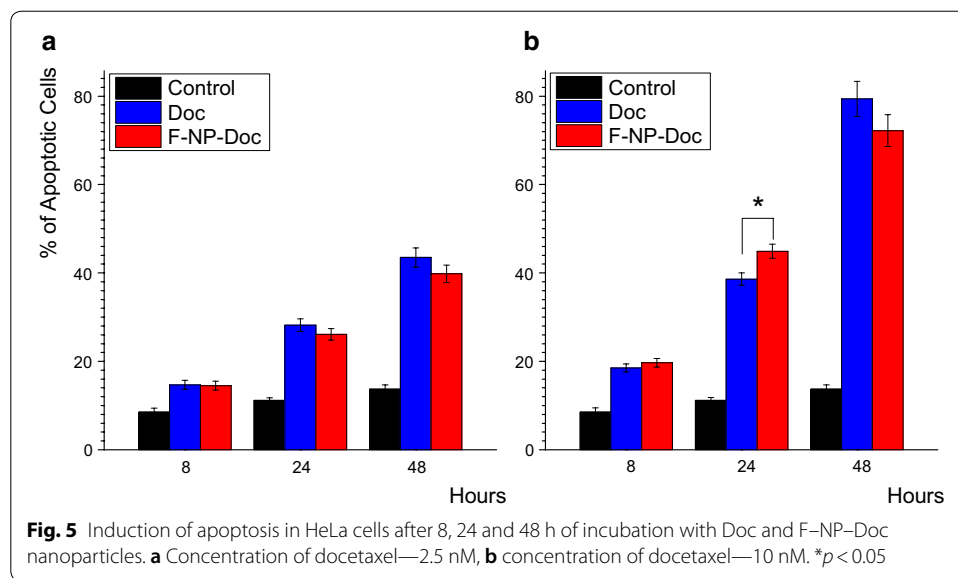


**Table 3** The cytostatic activity of F-NP-Doc versus free docetaxel expressed as IC<sub>50</sub> value

Incubation time, h	IC <sub>50</sub> , nM	
	Doc	F-NP-Doc
24	21.2 ± 2.0	9.3 ± 1.3
48	3.5 ± 0.4	2.5 ± 0.3
72	1.8 ± 0.2	1.0 ± 0.1

HeLa cells were incubated with F-NP-Doc and docetaxel for 24, 48 and 72 h. Cell survival was assessed using the SRB assay

of treatment with the drugs (Table 3) correlated with apoptosis induction detected by Annexin V staining at the same time points. PLGA nanoparticles without docetaxel, similarly formulated, showed no toxicity in the range of concentrations used (data not shown).

It was surprising to us that F-NP-Doc nanoparticles exhibited considerable activity against cancer cells even at short incubation times (8 and 24 h). It is well known that taxanes can easily pass through the cell membrane by diffusion due to their high hydrophobicity, while large polymeric particles enter the cell via macropinocytosis and receptor-mediated endocytosis (Behzadi et al. 2017; Rejman et al. 2004; Sahin et al. 2017), which are more time- and energy-consuming processes. In general, this causes a delay in the induction of cell death by docetaxel- and paclitaxel-loaded nanoparticles compared to free drug (Danhier et al. 2009). This might be the reason why authors sometimes do not provide comparative data on cytotoxicity of free drug and drug-loaded polymeric nanoparticles, since the obtained results are obviously not in favor of the latter (Chen et al. 2013; Ma et al. 2010). However, it should be kept in mind that docetaxel does not cause immediate cell death as this drug induces cytotoxicity by altering the rate and degree of microtubule polymerization and suppressing microtubule dynamics, which leads to inhibition of centrosome duplication in the S-phase (Paoletti et al. 1997), disruption of the mitotic spindle formation and

subsequent cell cycle arrest in S/G2/M phases (Hernandez-Vargas et al. 2007). Only thereafter, the cell death occurs by both apoptotic and non-apoptotic pathways.

It is logical to assume [and this assumption is confirmed by the experimental results reported (Adesina et al. 2014; Manoochchri et al. 2013; Patel et al. 2018; Pradhan et al. 2013; Ren et al. 2018), etc.] that the cytotoxic effect of docetaxel-loaded nanoparticles should manifest later than that of free docetaxel. However, in our experiments, as well as in some other studies, the reliability of which is beyond doubt (Kulhari et al. 2014; Noori Koopaei et al. 2014; Sanna et al. 2011), induction of apoptosis and death of cancer cells exposed to docetaxel-loaded nanoparticles were observed in a relatively short time. After 8 h of F-NP-Doc treatment at a concentration of 2.5 and 10 nM in docetaxel equivalent, the apoptotic cell population increased to 14.5% and 19.7%, respectively (Fig. 5). In turn, 2.5 and 10 nM of docetaxel generated 14.7% and 18.5% apoptotic cell population, respectively, at the same incubation time. When incubation period was prolonged from 8 to 24 h, a more pronounced induction of apoptosis was observed (26.1% and 43.4% for 2.5 and 10 nM of F-NP-Doc, respectively, while 28.2% and 38.6% for 2.5 and 10 nM of free docetaxel, respectively).

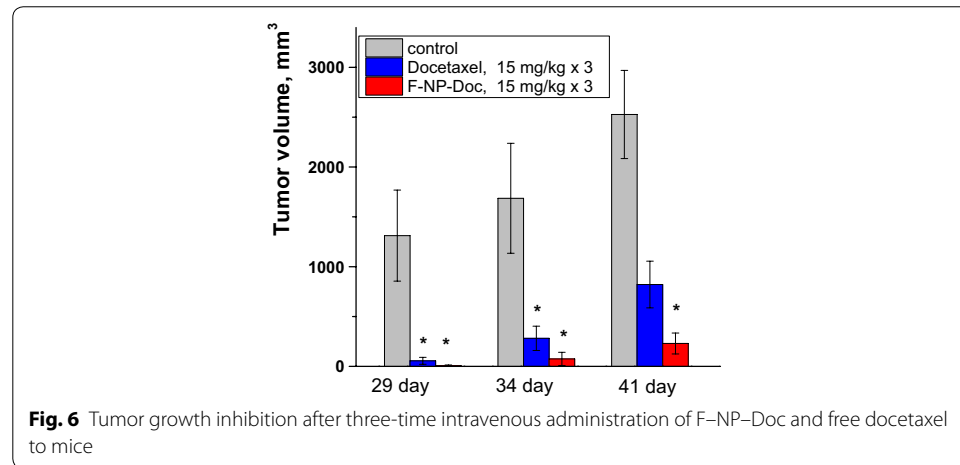
The IC<sub>50</sub> values for F-NP-Doc nanoparticles and free docetaxel in HeLa cells after 24 h of incubation were 9.3 nM and 21.2 nM, respectively. It is important to stress that although IC<sub>50</sub> values of both F-NP-Doc and free docetaxel decreased with an increase in incubation time, the cytostatic activity of F-NP-Doc significantly exceeded that of free drug at all times tested (Table 3). In vitro drug release study indicates a rather slow release of docetaxel from the polymer matrix (Fig. 2), as less than 20% from the initial content of docetaxel was released from F-NP-Doc nanoparticles during 24 h. However, due to the high docetaxel loading, this was sufficient to achieve effective intracellular drug concentration and to exhibit significantly higher anticancer activity than free docetaxel. Additionally, incorporation of docetaxel into polymeric nanoparticles improves its stability, which may also be of great importance. It is known that docetaxel is unstable in aqueous solutions due to the presence of *N*-tert-butyl group on the synthetic side chain of the molecule (Tian and Stella 2008). Oxidation of this moiety significantly reduces the ability of docetaxel to interact with microtubule  $\beta$ -tubulin (Grover et al. 1995). In turn, permeation of water into PLGA nanoparticles is hindered, so docetaxel loaded into them remains intact and enters the cell in its natural state.

We carried out a comparative analysis of the cytostatic activity of F-NP-Doc and free docetaxel against cancer and normal cell lines. The results suggest that the targeted nanoparticles inhibit HeLa cell growth more potently than free docetaxel as assessed by IC<sub>50</sub>. In contrast, F-NP-Doc were five times less toxic to LECH human embryonic lung fibroblasts (control cells with low expression of folate receptors) than the free drug (Fig. 4b). LECH cells were nine times more resistant to F-NP-Doc than HeLa cells, while both lines demonstrated the same sensitivity to docetaxel. These data indicate that the targeted F-NP-Doc nanoparticles selectively kill cancer cells that overexpress folate receptors.

To confirm the “targetability” of F-NP-Doc nanoparticles, we investigated their activity towards MCF7<sup>R</sup> breast adenocarcinoma cells with overexpression of Pgp170 glycoprotein (Batrakova et al. 2001). It is known that this glycoprotein belongs to the family of ABC-transporters and is responsible for decreased intracellular accumulation of

**Table 4** The cytostatic activity of F-NP-Doc and free docetaxel against cancer cells expressed as IC<sub>50</sub> value  $\pm$  SE

Drug	Cells						
	HeLa	MCF7	MCF7 <sup>R</sup>	MDA-MB-231	SKOV3	Ca755	LECH
Docetaxel	2.9 $\pm$ 0.4	7.7 $\pm$ 1.2	166 $\pm$ 15.3	0.5 $\pm$ 0.03	3.2 $\pm$ 0.4	9.7 $\pm$ 2.6	2.2 $\pm$ 1.9
F-NP-Doc	1.2 $\pm$ 0.3	4.9 $\pm$ 0.6	65 $\pm$ 8.3	1.8 $\pm$ 0.6	2.0 $\pm$ 0.4	5.6 $\pm$ 0.7	11.2 $\pm$ 2.2



various anticancer agents including docetaxel (Noguchi 2006). We found that docetaxel and non-targeted docetaxel-loaded nanoparticles exhibited a similar cytostatic activity against MCF7<sup>R</sup> cells, with IC<sub>50</sub> being 163 and 166 nM, respectively. On the contrary, F-NP-Doc reversed, at least partially, multidrug resistance in MCF7<sup>R</sup> cells and more effectively decreased their survival, with IC<sub>50</sub> being 65 nM (Fig. 4d).

The efficacy of F-NP-Doc NPs varied depending on the folate receptor expression levels in cells (Tables 2, 4).

### In vivo anticancer efficacy

To study the antitumor activity of F-NP-Doc-targeted nanoparticles in vivo, we established the syngeneic mouse model by serial subcutaneous transplantation of tumors arising from Ca755 mammary adenocarcinoma cells into female C57BL/6 mice. F-NP-Doc and free docetaxel were intravenously administered every 72 h (three injections). The results of the study of F-NP-Doc antitumor activity are shown in Fig. 6. Significant inhibition of tumor growth was observed after F-NP-Doc administration at a dosage of 15 mg/kg/dose. Moreover, the antitumor effect of F-NP-Doc was higher compared to that of docetaxel throughout the observation period up to 41 days (32 days after treatment was finished). Comparison of TGI for F-NP-Doc and docetaxel on days 25–41 showed that TGI for F-NP-Doc remained at a high level (from 100 to 90.9%) during this period, while TGI for docetaxel decreased from 99.9 to 67.5%. These results suggest that F-NP-Doc exhibit higher in vivo antitumor activity and more profoundly reduce the tumor volume compared to free docetaxel.

## Conclusion

In this study, we investigated the biological activity of folate-modified docetaxel-loaded PLGA nanoparticles prepared by a single-emulsion solvent-evaporation method. The targeted nanoparticles showed higher in vitro anticancer activity towards HeLa cervical carcinoma cells and MCF7 breast adenocarcinoma cells than both non-functionalized nanoparticles and free docetaxel. Meanwhile, the toxicity of targeted nanoparticles to human fibroblasts was nine times lower. F-NP-Doc nanoparticles as well as free docetaxel induced apoptosis in cancer cells. F-NP-Doc, but not non-targeted PLGA nanoparticles, reversed multidrug resistance in MCF7<sup>R</sup> breast adenocarcinoma cells. A pronounced anticancer effect of folate-modified docetaxel-loaded PLGA nanoparticles was attributed to an increase in availability of docetaxel to cancer cells and targeted intracellular delivery. High antitumor activity of F-NP-Doc has also been proven in in vivo experiments.

## Abbreviations

BSA: bovine serum albumin; DLS: dynamic light scattering; DMEM: Dulbecco's Modified Eagle Medium; DMSO: dimethyl sulfoxide; Doc: docetaxel; EDTA: ethylenediaminetetraacetic acid; FA: folic acid; FBS: fetal bovine serum; FITC: fluorescein isothiocyanate; F-NP-FDA: folate-modified fluorescein diacetate-loaded PLGA nanoparticles; F-NP-Doc: folate-modified docetaxel-loaded PLGA nanoparticles; FoAD: folic acid-dodecylamine; G2: Gap2 phase of cell cycle; HPLC: high-performance liquid chromatography; IC50: the half maximal inhibitory concentration; M: mitosis; MeCl<sub>2</sub>: methylene chloride; MFI: medium fluorescence intensity; MTT: 3-(4,5-dimethyl-2-thiazolyl)-2,5-diphenyl-2H-tetrazolium bromide; NP-Doc: docetaxel-loaded PLGA nanoparticles; NPs: nanoparticles; PBS: phosphate buffered saline; Pdl: polydispersity index; PI: propidium iodide; PLGA: poly(D,L-lactic-co-glycolic acid); PVA: polyvinyl alcohol; S phase: synthesis phase of cell cycle; SE: standard error; SI: staining index; SRB: sulforhodamine B; TEM: transmission electron microscopy.

## Acknowledgements

The authors are grateful to the resource center "Molbiotekh" NRC "Kurchatov Institute" for the equipment provided to perform this work. The authors thank Dr. M. Ratushnyak for assistance in conducting experiments, E. B. Pichkur for assistance in electron microscopy, and Dr. N. Gukasova for critically revising the manuscript.

## Authors' contributions

YIP devised the overall project, prepared the nanoparticles, organized data analysis and described materials and methods. VVZ performed in vitro drug release studies and data analysis. ASZ, YPS and VGS participated in cell culture experiments, and ASZ analyzed and organized the results. YPS carried out flow cytometry measurements and helped in writing the manuscript. SVA carried out the HPLC analysis. DOD determined the particle size and zeta potential, and interpreted the results. AAK performed in vivo experiments. EAV and VYB participated in the experimental set-up development as well as discussion and data analysis. GAP designed and coordinated this study, supervised the findings and wrote the entire manuscript. All authors read and approved the final manuscript.

## Funding

This study was supported by Ministry of Education and Science of the Russian Federation as a part of the Federal Targeted Programme for Research and Development in Priority Areas of Advancement of the Russian Scientific and Technological Complex for 2014–2020, Agreement No. 14.607.21.0198. The unique identifier: RFMEFI60717X0198.

## Availability of data and materials

All data generated or analyzed during this study are included in this published article.

## Ethics approval and consent to participate

All animal experiments were carried out in accordance with the European Convention for the Protection of Vertebrate Animals (Strasbourg 1986). The protocols of this study and experimental procedures were approved by the Ethical Committee of the National Research Center "Kurchatov Institute".

## Consent for publication

Consent given to corresponding author on behalf of all other authors.

## Competing interests

The authors declare that they have no competing interests.

## Author details

<sup>1</sup> National Research Centre "Kurchatov Institute", Moscow 123182, Russia. <sup>2</sup> Lomonosov Moscow State University, Moscow 119991, Russia.

Received: 20 November 2018 Accepted: 28 April 2019

Published online: 13 May 2019

## References

- Adesina SK, Holly A, Kramer-Marek G, Capala J, Akala EO. Polylactide-based paclitaxel-loaded nanoparticles fabricated by dispersion polymerization: characterization, evaluation in cancer cell lines, and preliminary biodistribution studies. *J Pharm Sci*. 2014;103(8):2546–55. <https://doi.org/10.1002/jps.24061>.
- Alley MC, Scudiero DA, Monks A, Hursey ML, Czerwinski MJ, Fine DL, et al. Feasibility of drug screening with panels of human tumor cell lines using a microculture tetrazolium assay. *Cancer Res*. 1988;48(3):589–601.
- Bareford LM, Swaan PW. Endocytic mechanisms for targeted drug delivery. *Adv Drug Deliv Rev*. 2007;59(8):748–58. <https://doi.org/10.1016/j.addr.2007.06.008>.
- Batrakova EV, Li S, Elmquist WF, Miller DW, Alakhov VY, Kabanov AV. Mechanism of sensitization of MDR cancer cells by Pluronic block copolymers: selective energy depletion. *Br J Cancer*. 2001;85(12):1987–97. <https://doi.org/10.1054/bjoc.2001.2165>.
- Behzadi S, Serpooshan V, Tao W, Hamaly MA, Alkawareek MY, Dreaden EC, et al. Cellular uptake of nanoparticles: journey inside the cell. *Chem Soc Rev*. 2017;46(14):4218–44. <https://doi.org/10.1039/c6cs00636a>.
- Chattopadhyay S, Dash SK, Ghosh T, Das D, Pramanik P, Roy S. Surface modification of cobalt oxide nanoparticles using phosphonomethyl iminodiacetic acid followed by folic acid: a biocompatible vehicle for targeted anticancer drug delivery. *Cancer Nanotechnol*. 2013;4(4):103–16. <https://doi.org/10.1007/s12645-013-0042-7>.
- Chen Y, Yang Z, Liu C, Wang C, Zhao S, Yang J, et al. Synthesis, characterization, and evaluation of paclitaxel loaded in six-arm star-shaped poly(lactic-co-glycolic acid). *Int J Nanomed*. 2013;8:4315–26. <https://doi.org/10.2147/IJN.S51629>.
- Danhier F, Lecouturier N, Vroman B, Jerome C, Marchand-Brynaert J, Feron O, et al. Paclitaxel-loaded PEGylated PLGA-based nanoparticles: in vitro and in vivo evaluation. *J Control Release*. 2009;133(1):11–7. <https://doi.org/10.1016/j.jconrel.2008.09.086>.
- Eisenhauer EA, Vermorken JB. The taxoids. Comparative clinical pharmacology and therapeutic potential. *Drugs*. 1998;55(1):5–30. <https://doi.org/10.2165/00003495-199855010-00002>.
- Grover S, Rimoldi JM, Molinero AA, Chaudhary AG, Kingston DG, Hamel E. Differential effects of paclitaxel (Taxol) analogs modified at positions C-2, C-7, and C-3' on tubulin polymerization and polymer stabilization: identification of a hyperactive paclitaxel derivative. *Biochemistry*. 1995;34(12):3927–34. <https://doi.org/10.1021/bi00012a009>.
- Gurski LA, Jha AK, Zhang C, Jia X, Farach-Carson MC. Hyaluronic acid-based hydrogels as 3D matrices for in vitro evaluation of chemotherapeutic drugs using poorly adherent prostate cancer cells. *Biomaterials*. 2009;30(30):6076–85. <https://doi.org/10.1016/j.biomaterials.2009.07.054>.
- Hernandez-Vargas H, Palacios J, Moreno-Bueno G. Telling cells how to die: docetaxel therapy in cancer cell lines. *Cell Cycle*. 2007;6(7):780–3. <https://doi.org/10.4161/cc.6.7.4050>.
- Hoshyar N, Gray S, Han H, Bao G. The effect of nanoparticle size on in vivo pharmacokinetics and cellular interaction. *Nanomedicine*. 2016;11(6):673–92. <https://doi.org/10.2217/nnm.16.5>.
- Huang J, Bu L, Xie J, Chen K, Cheng Z, Li X, et al. Effects of nanoparticle size on cellular uptake and liver MRI with polyvinylpyrrolidone-coated iron oxide nanoparticles. *ACS Nano*. 2010;4(12):7151–60. <https://doi.org/10.1021/nn101643u>.
- Kamaly N, Yameen B, Wu J, Farokhzad OC. Degradable controlled-release polymers and polymeric nanoparticles: mechanisms of controlling drug release. *Chem Rev*. 2016;116(4):2602–63. <https://doi.org/10.1021/acs.chemrev.5b00346>.
- Kapoor DN, Bhatia A, Kaur R, Sharma R, Kaur G, Dhawan S. PLGA: a unique polymer for drug delivery. *Ther Deliv*. 2015;6(1):41–58. <https://doi.org/10.4155/tde.14.91>.
- Kraus LA, Samuel SK, Schmid SM, Dykes DJ, Waud WR, Bissery MC. The mechanism of action of docetaxel (Taxotere) in xenograft models is not limited to bcl-2 phosphorylation. *Invest New Drugs*. 2003;21(3):259–68. <https://doi.org/10.1023/A:1025436307913>.
- Kulhari H, Pooja D, Shrivastava S, Naidu VG, Sistla R. Peptide conjugated polymeric nanoparticles as a carrier for targeted delivery of docetaxel. *Colloids Surf B*. 2014;117:166–73. <https://doi.org/10.1016/j.colsurfb.2014.02.026>.
- Li SM. Hydrolytic degradation characteristics of aliphatic polyesters derived from lactic and glycolic acids. *J Biomed Mater Res*. 1999;48(3):342–53. [https://doi.org/10.1002/\(sici\)1097-4636\(1999\)48:3%3C342::aid-jbm20%3e3.0.co;2-7](https://doi.org/10.1002/(sici)1097-4636(1999)48:3%3C342::aid-jbm20%3e3.0.co;2-7).
- Lim HA, Raku T, Tokiwa Y. Hydrolysis of polyesters by serine proteases. *Biotechnol Lett*. 2005;27(7):459–64. <https://doi.org/10.1007/s10529-005-2217-8>.
- Liu X, Huang N, Li H, Jin Q, Ji J. Surface and size effects on cell interaction of gold nanoparticles with both phagocytic and nonphagocytic cells. *Langmuir*. 2013;29(29):9138–48. <https://doi.org/10.1021/la401556k>.
- Lu F, Wu S-H, Hung Y, Mou C-Y. Size effect on cell uptake in well-suspended, uniform mesoporous silica nanoparticles. *Small*. 2009;5(12):1408–13. <https://doi.org/10.1002/smll.200900005>.
- Ma Y, Zheng Y, Liu K, Tian G, Tian Y, Xu L, et al. Nanoparticles of poly(lactide-co-glycolide)-d- $\alpha$ -tocopheryl polyethylene glycol 1000 succinate random copolymer for cancer treatment. *Nanoscale Res Lett*. 2010;5(7):1161–9. <https://doi.org/10.1007/s11671-010-9620-3>.
- Manoochehri S, Darvishi B, Kamalinia G, Amini M, Fallah M, Ostad SN, et al. Surface modification of PLGA nanoparticles via human serum albumin conjugation for controlled delivery of docetaxel. *Daru*. 2013;21(1):58. <https://doi.org/10.1186/2008-2231-21-58>.
- Mohammad AK, Reineke JJ. Quantitative detection of PLGA nanoparticle degradation in tissues following intravenous administration. *Mol Pharm*. 2013;10(6):2183–9. <https://doi.org/10.1021/mp300559v>.
- Montero A, Fossella F, Hortobagyi G, Valero V. Docetaxel for treatment of solid tumours: a systematic review of clinical data. *Lancet Oncol*. 2005;6(4):229–39. [https://doi.org/10.1016/S1470-2045\(05\)70094-2](https://doi.org/10.1016/S1470-2045(05)70094-2).
- Noguchi S. Predictive factors for response to docetaxel in human breast cancers. *Cancer Sci*. 2006;97(9):813–20. <https://doi.org/10.1111/j.1349-7006.2006.00265.x>.
- Noori Koopaei M, Khoshayand MR, Mostafavi SH, Amini M, Khorramizadeh MR, Jeddi Tehrani M, et al. Docetaxel loaded PEG-PLGA nanoparticles: optimized drug loading, in-vitro cytotoxicity and in-vivo antitumor effect. *Iran J Pharm Res IJPR*. 2014;13(3):819–33. <https://doi.org/10.22037/IJPR.2014.1533>.
- Paoletti A, Giocanti N, Favaudon V, Bornens M. Pulse treatment of interphasic HeLa cells with nanomolar doses of docetaxel affects centrosome organization and leads to catastrophic exit of mitosis. *J Cell Sci*. 1997;110:2403–15.



- Parveen S, Sahoo SK. Evaluation of cytotoxicity and mechanism of apoptosis of doxorubicin using folate-decorated chitosan nanoparticles for targeted delivery to retinoblastoma. *Cancer Nanotechnol.* 2010;1(1):47–62. <https://doi.org/10.1007/s12645-010-0006-0>.
- Patel J, Amrutiya J, Bhatt P, Javia A, Jain M, Misra A. Targeted delivery of monoclonal antibody conjugated docetaxel loaded PLGA nanoparticles into EGFR overexpressed lung tumour cells. *J Microencapsul.* 2018;35(2):204–17. <https://doi.org/10.1080/02652048.2018.1453560>.
- Pradhan R, Poudel BK, Ramasamy T, Choi HG, Yong CS, Kim JO. Docetaxel-loaded polylactic acid-co-glycolic acid nanoparticles: formulation, physicochemical characterization and cytotoxicity studies. *J Nanosci Nanotechnol.* 2013;13(8):5948–56. <https://doi.org/10.1166/jnn.2013.7735>.
- Rejman J, Oberle V, Zuhorn IS, Hoekstra D. Size-dependent internalization of particles via the pathways of clathrin- and caveolae-mediated endocytosis. *Biochem J.* 2004;377:159–69. <https://doi.org/10.1042/BJ20031253>.
- Ren G, Chen P, Tang J, Wang R, Duan S, Wang R, et al. Construction and cellular uptake evaluation of redox-responsive docetaxel prodrug self-assembled nanoparticles. *Drug Dev Ind Pharm.* 2018;44(4):598–607. <https://doi.org/10.1080/03639045.2017.1405435>.
- Sahin A, Esendagli G, Yerlikaya F, Caban-Toktas S, Yoyen-Ermis D, Horzum U, et al. A small variation in average particle size of PLGA nanoparticles prepared by nanoprecipitation leads to considerable change in nanoparticles' characteristics and efficacy of intracellular delivery. *Artif Cells Nanomed Biotechnol.* 2017;45(8):1657–64. <https://doi.org/10.1080/21691401.2016.1276924>.
- Sanna V, Roggio AM, Posadino AM, Cossu A, Marceddu S, Mariani A, et al. Novel docetaxel-loaded nanoparticles based on poly(lactide-co-caprolactone) and poly(lactide-co-glycolide-co-caprolactone) for prostate cancer treatment: formulation, characterization, and cytotoxicity studies. *Nanoscale Res Lett.* 2011;6(1):260. <https://doi.org/10.1186/1556-276x-6-260>.
- Skehan P, Storeng R, Scudiero D, Monks A, McMahon J, Vistica D, et al. New colorimetric cytotoxicity assay for anticancer-drug screening. *J Natl Cancer Inst.* 1990;82(13):1107–12. <https://doi.org/10.1093/jnci/82.13.1107>.
- Suriamoorthy P, Zhang X, Hao G, Joly AG, Singh S, Hossu M, et al. Folic acid-CdTe quantum dot conjugates and their applications for cancer cell targeting. *Cancer Nanotechnol.* 2010;1(1–6):19–28. <https://doi.org/10.1007/s12645-010-0003-3>.
- Syu WJ, Yu HP, Hsu CY, Rajan YC, Hsu YH, Chang YC, et al. Improved photodynamic cancer treatment by folate-conjugated polymeric micelles in a KB xenografted animal model. *Small.* 2012;8(13):2060–9. <https://doi.org/10.1002/sml.201102695>.
- Tian J, Stella VJ. Degradation of paclitaxel and related compounds in aqueous solutions II: nonepimerization degradation under neutral to basic pH conditions. *J Pharm Sci.* 2008;97(8):3100–8. <https://doi.org/10.1002/jps.21214>.
- Tsuji T, Yoshitomi H, Usukura J. Endocytic mechanism of transferrin-conjugated nanoparticles and the effects of their size and ligand number on the efficiency of drug delivery. *Microscopy.* 2013;62(3):341–52. <https://doi.org/10.1093/jmicr/dfs080>.
- Wang F, Chen Y, Zhang D, Zhang Q, Zheng D, Hao L, et al. Folate-mediated targeted and intracellular delivery of paclitaxel using a novel deoxycholic acid-O-carboxymethylated chitosan-folic acid micelles. *Int J Nanomed.* 2012;7:325–37. <https://doi.org/10.2147/ijn.s27823>.
- Wu W, Zheng Y, Wang R, Huang W, Liu L, Hu X, et al. Antitumor activity of folate-targeted, paclitaxel-loaded polymeric micelles on a human esophageal EC9706 cancer cell line. *Int J Nanomed.* 2012;7:3487–502. <https://doi.org/10.2147/ijn.s32620>.
- Ye W-L, Du J-B, Zhang B-L, Na R, Song Y-F, Mei Q-B, et al. Cellular uptake and antitumor activity of DOX-hyd-PEG-FA nanoparticles. *PLoS ONE.* 2014;9(5):e97358. <https://doi.org/10.1371/journal.pone.0097358>.
- Yu C, Hu Y, Duan J, Yuan W, Wang C, Xu H, et al. Novel aptamer-nanoparticle bioconjugates enhances delivery of anticancer drug to MUC1-positive cancer cells in vitro. *PLoS ONE.* 2011;6(9):e24077. <https://doi.org/10.1371/journal.pone.0024077>.

## Publisher's Note

Springer Nature remains neutral with regard to jurisdictional claims in published maps and institutional affiliations.

**Ready to submit your research? Choose BMC and benefit from:**

- fast, convenient online submission
- thorough peer review by experienced researchers in your field
- rapid publication on acceptance
- support for research data, including large and complex data types
- gold Open Access which fosters wider collaboration and increased citations
- maximum visibility for your research: over 100M website views per year

**At BMC, research is always in progress.**

Learn more [biomedcentral.com/submissions](https://biomedcentral.com/submissions)

